Peer-reviewed version available at Appl. Sci. 2018, 8, 1121; doi:10.3390/app8071121

(Article)

A Quantitative Structure-activity Relationships Model Based on Hybrid Artificial Intelligence Methods and its Application

Mengshan Li* Huaijin Zhang, Liang Liu, Bingsheng Chen, Lixin Guan and Yan Wu

College of Physics and Electronic Information, Gannan Normal University, Ganzhou, Jiangxi 341000, China;
* Correspondence: jcimsli@163.com, lms@gnnu.cn ; Tel.: +86-797-8393668

Featured Application: The proposed hybrid intelligent model can be applied in all kinds of engineering design, material performance prediction, numerical calculation, prediction of physical and chemical properties and intelligent calculation.

Abstract: Quantitative structure-activity relationship (QSAR) model is adopted to study the relationship between the chemical and physical properties of various substances and the structure. Through QSAR studies, the internal relationship between the invisible structure and the activity can be obtained. In this paper, a novel chaos-enhanced accelerate particle swarm algorithm (CAPSO) is proposed, which is used to molecular descriptors screening and optimization of the weights of back propagation artificial neural network (BP ANN). Then, the QSAR model based on CAPSO and BP ANN is put forward, hereinafter referred to as CAPSO BP ANN model. The prediction experiment showed that the CAPSO algorithm is a reliable method for screening molecular descriptors and the five molecular descriptors obtained by CAPSO algorithm could well characterize the molecular structure of each compound in pKa prediction. The experimental results also showed the CAPSO BP ANN model has a good performance in predicting the pKa values of various compounds, the absolute mean relative error, root mean square error, and square correlation coefficient are respectively 0.5364, 0.0632, and 0.9438, indicating the higher prediction accuracy and correlation. The proposed hybrid intelligent model can be applied in all kinds of engineering design, prediction of physical and chemical properties and intelligent calculation.

Keywords: quantitative structure-activity relationship; hybrid intelligence; artificial neural network; particle swarm optimization

1. Introduction

In quantitative structure-activity relationship (QSAR) modeling, some calculation methods such as mathematical statistics, machine learning method and artificial intelligence method are used to explore the chemical and physical properties of various substances, it is a set of methods reflecting the relationship between activity and structure. Through the QSAR studies, the internal relationship between the invisible structure and the activity can be excavated[1,2]. QSAR study can be used to predict the activity of unknown materials and discover key influencing factors of the activity of related substances, such as groups or substituents determining the activity of the molecular structure[3,4]. Nowadays, QSAR has been applied in the fields of computer science, chemistry, materials science, medicine science, and life sciences[5,6].

The establishment of QSAR model mainly involves the following steps: the acquisition of experimental data, the construction and optimization of the molecular structure, the calculation and screening of molecular descriptors, the establishment and verification of the model, etc. First of all, the selection of molecular descriptors plays a decisive role in the quality of QSAR

model. The screening step aims to reflect more structural information with the less molecular structure descriptors as possible. Many methods have been developed to screen molecular descriptors and can be mainly divided into two categories[7-9], traditional variable selection methods (such as the PLS method and its variants) and modern search algorithms based on the optimization strategy (genetic algorithm GA, simulated annealing algorithm SA, ant colony algorithm AC, particle swarm optimization PSO, and other swarm intelligence algorithms)[10-12]. Traditional variable selection methods are the most simple and efficient and can quickly screen descriptors, but their overall performances are low especially in the complex nonlinear data collection. The modern search algorithms based on the optimization strategy have obvious advantages and can search for optimal variables and deal with complex large data sets. The model establishment is important in the QSAR study and commonly used QSAR models include two-dimensional(2d) , three-dimensional (3d), four-dimensional(4d), and five-dimension(4d)[13-15]. According to the modeling ideas, these methods can be divided into linear and nonlinear QSAR methods. Linear methods mainly include multiple regression methods (MLR), partial least squares (PLS), and principal component methods[16], nonlinear methods include support vector machine and artificial neural network (ANN) method[17-21].

However, the QSAR study based on various artificial intelligence algorithms also has some shortcomings, such as high computational complexity and low prediction accuracy[22]. Therefore, it is necessary to develop the QSAR model with high accuracy, high efficiency and good stability. In this paper, a novel QSAR modeling is proposed based on BP ANN and the accelerated particle swarm algorithm (APSO) reported in recent years, an improved APSO is used to molecular descriptors screening and optimization of the weights of BP ANN. Then, the QSAR modeling is used to predict pKa values of various compounds combined with others artificial neural networks.

2. Modeling theory and Methods

2.1 Chaos-enhanced accelerated particle swarm optimization algorithm

Particle Swarm Optimization (PSO) was proposed by Eberhart and Kennedy[23] in 1995, but the performance of the standard PSO algorithm is not high enough and shows some defects, such as parameter sensitivity, premature convergence, and slow local search. In recent years, a variant PSO called accelerated PSO (APSO) has attracted wide attention from scholars[24-27]. Although the APSO improves the convergence speed, the algorithm also may lead to premature convergence and omit some extreme values. Therefore, in the study, we propose a new chaos-enhanced accelerated particle swarm optimization algorithm (CAPSO) by integrating chaos theory into the improvement of APSO algorithm.

In the APSO algorithm, the influences of inertial weight factor or cognitive factor on the particle is not considered, and the algorithm is improved with only the global exploration factor[28]. The main idea of the algorithm is to fully rights to the variable that is responsible for global search, and considering the update of the particle with the exploration factor. In the whole search process, the particle is only constrained by the global extreme value. The position update formula is:

$$x_{i,d}^{k+1} = (1 - C_2)x_{i,d}^{k} + C_2 p_{g,d}^{k} + C_1 r, \quad (1)$$

where C_1 and C_2 are learning factors; r is the random number between 0 and 1; $x_{i,d}^{k}$ is the position of particle i in d-dimensional kth iteration; $p_{g,d}^{k}$ is the position of the global extremum of the whole population in d-dimension.

Compared with the standard PSO algorithm, APSO uses two parameters C_1 and C_2, to reduce the randomness in the iterative process. In this paper, C_1 represents the monotonically decreasing function: $C_1 = \delta^t$, where $0 < \delta < 1$ and t is the current iteration number. Therefore, the performance of the APSO algorithm is mainly affected by parameter C_2. For common problems, the value is [0.2,0.7]. When C_2 is 1, the particle can converge at any time to the current global value and

no longer changes, and the global value may not be the real global value at all; on the contrary, when C_2 is 0, the global search speed of the algorithm is extremely slow. Therefore, it is very important for the optimization of C_2. In this paper, the classical logistic equation is used to realize the evolution of chaotic variables and optimize the parameters. The iterative formula is as follows:

$$x_i^{k+1} = 4x_i^k(1 - x_i^k), \quad (2)$$

when $0 < x_i^k < 1$, logistic equation is in a completely chaotic state.

The CAPSO algorithm involves the following steps:

Step 1: To initialize the particle group. The particles in PSO algorithm are initialized. The optimal value of the individual extremum is selected as the global optimal value to generate chaotic values;

Step 2: To calculate the adaptive value of group particles;

Step 3: The adaptive value of each particle is compared with the best value itself. If the adaptive value is better, update the best position;

Step 4: The learning factor C2 is obtained from the chaotic sequence (generated by Eq. (2)) and the position of the particle is updated with Eq. (1);

Step 5: If the end condition of the algorithm is satisfied, the global optimum position is the optimal solution. The result is saved and the algorithm is completed. Otherwise, return to Step 2.

2.2 QSAR model based on the hybrid intelligent method

The back propagation artificial neural network (BP ANN) is one of the most important network models. It usually consists of input layer, hidden layer, and output layere[29-31]. The implementation of BP ANN mainly consists of two processes: learning process and working process[32,33].

In a three-layer BP ANN, each layer consists of several nodes. The input layer receives input information of the network. Then, the input information is processed and sent to the hidden layer. The relationship between input and output can be expressed as:

Input: $net = x_1w_1 + x_2w_2 + \cdots x_nw_n$

Output: $y = f(net) = \dfrac{1}{1+e^{-net}}$

where $x_1, x_2, \cdots x_n$ are the input vectors of the network; $w_1, w_2, \cdots w_n$ are the connection weights for each input vector; y is the output of the network.

In BP ANN model, the nonlinear relationship between input and output is established by determining the weight and deviation between each layer. Structurally, the nonlinear relationship between the input and output can be understood as: output $y = f(w_{ih}, w_{ho}, b_o)$, where w_{ih}, w_{ho}, b_o are respectively the weight vector between the input layer and the hidden layer, the weight vector between the hidden layer and the output layer, and the deviation vector of the hidden layer. The performance of the network depends on the three main parameters of the network (w_{ih}, w_{ho}, b_o).

To improve BP algorithm, a prediction model based on CAPSO and BP ANN, called CAPSO BP ANN, is proposed by optimizing BP ANN parameters with the CAPSO algorithm. The CAPSO BP ANN model makes full use of the strong global search capability of PSO algorithm and the fast local search capability of BP algorithm, thus improving the prediction speed and accuracy of the model. In CAPSO BP ANN, PSO algorithm was proposed to optimize BP ANN parameters w_{ih}, w_{ho}, b_o. Therefore, in the PSO optimization algorithm, the particle is designed as the structure of weight vector w_{ih}, weight vector w_{ho} and deviation vector b_o:

$$particle(i) = [w_{ih}, w_{ho}, b_o]. \quad (3)$$

The implementation of the CAPSO BP ANN model can be simply described as follows:

Step 1: To initialize the model. The connection weights, deviations and population parameters of the model are initialized by the random method;

Preprints (www.preprints.org) | NOT PEER-REVIEWED | Posted: 31 May 2018 doi:10.20944/preprints201805.0475.v1

Peer-reviewed version available at Appl. Sci. 2018, 8, 1121; doi:10.3390/app8071121

Step 2: Model training. The PSO algorithm is used to optimize the parameters of BP ANN and the particle structure is designed above.

Step 3: Parameter adjustment. Based on the error of output, the parameters are adjusted until the number of execution times reaches the set value or the error satisfies the setting condition.

Step 4: Output. After training, the model outputs each parameter and then the trained model is tested.

2.3 Model evaluation

The evaluation of the model is mainly based on the stability and reliability of the model. In this paper, the evaluation indices of prediction accuracy including the absolute average relative deviation (*AARD*) and the root mean square error of prediction (*RMSEP*) are defined as follows:

$$AARD = \frac{1}{N}\sum_{i=1}^{N}\frac{\left|\overline{y}_i - y_i\right|}{y_i}; \tag{4}$$

$$RMSEP = \sqrt{\frac{1}{N}\sum_{i=1}^{N}(y_i - \overline{y}_i)^2}\ . \tag{5}$$

Squared correlation coefficient (R^2) can reflect the correlation between predicted values and experimental values and defined as follows:

$$R^2 = \frac{\left[\sum_{i=1}^{N}(y_i - y_{ave})(\overline{y}_i - \overline{y}_{ave})\right]^2}{\sum_{i=1}^{N}(y_i - y_{ave})^2\sum_{i=1}^{N}(\overline{y}_i - \overline{y}_{ave})^2}. \tag{6}$$

In these formulas, N is the number of samples; $\overline{y}_i$ is the predicted or calculated value of the model; y_i is the actual value obtained in experiments; y_{ave} is the average of actual values of the samples; $\overline{y}_{ave}$ is the average of predicted values.

3. Experimental study

This section may be divided by subheadings. It should provide a concise and precise description of the experimental results, their interpretation as well as the experimental conclusions that can be drawn.

3.1 Experimental data

The comprehensive performance of the model was verified by predicting the pKa value of the compound. The experimental database source is shown in Table 1. The database consists of 268 sets of data. In order to obtain a more reasonable prediction model, the database is randomly divided into three subsets of training set, verification set, and testing set. The training set is used to establish the model. The verification set is used to optimize and validate the model. The testing set is used to test the performance of the model and the tested performance can directly reflect the comprehensive performance of the model.

Table 1 Statistical table of experimental data

Number of Compounds	Experimental *pKa*	Reference
31	0.70-4.99	[34,35]
34	5.00-6.99	[34-36]
16	7.00-7.99	[34-36]
46	8.00-8.99	[34-36]

Number of Compounds	Experimental *pKa*	Reference
80	9.00-9.99	[34-36]
45	10.00-10.99	[34-36]
16	11.00-13.80	[34,35]

In this paper, 70% of the data are used for training. Both verification set and testing set account for 15%. The number of the experimental data in training set, validation set and testing set are respectively 188, 40, and 40.

3.2 Screening of molecular descriptors

The molecular descriptors are generated by the following methods:

- Construction of molecular structure. It is obtained in the Chemdraw UItra 7.0 software.
- Optimization of molecular structure. The molecular structure is further optimized in Hyper Chem 7.5 software.
- Calculation of molecular descriptors. The optimized molecular structure is imported into CODESSA software and the corresponding molecular descriptors are obtained by calculation.

Through molecular descriptor computing software, 733 molecular descriptors are generated, some of the molecular descriptors are closely related to each other. When modeling, it is necessary to filter a large number of calculated molecular descriptors in order to select the descriptors which are the most closely related to the research questions. The quality of the QSAR model depends on the way to determine molecular descriptors to a large extent.

In this study, CAPSO algorithm is used to screen a large number of calculated molecular descriptors. The implementation process of filtering molecular descriptors with CAPSO is described as follows:

Step 1. Population initialization. To set the population size and initialize the population individual as a molecular descriptor; to set the evolutionary counter and the maximum number of iterations.

Step 2. Adaptive evaluation. To calculate the fitness of all the molecular descriptors of a population.

Step 3. Molecular descriptor selection. To select the next generation of molecular descriptors based on individual fitness values.

Step 4. Population renewal. To iterate over the molecular descriptors in the population and get the next generation of molecular descriptor population.

Step 5. Re-evaluation of individual adaptive values. To calculate the fitness of all the molecular descriptors of the population through iterative evolution and re-evaluate the merits and demerits of the individuals.

Step 6. Iteration. To judge whether the iteration condition is satisfied. If it is satisfied, the evolution is ended, otherwise turn to Step 3 and continue iteration.

Finally, five molecular descriptors were selected through CAPSO's search for molecular descriptors (Table 2).

Table 2 Molecular descriptors selected by CAPSO algorithm

No.	Molecular descriptors	Descriptor types
1	Relative number of N atoms	Constitutional descriptors
2	Randic index (order 3)	Topological descriptors
3	RNCG relative negative charged (QMNEG/QTMINUS) [Quantum-Chemical PC]	Electrostatic descriptors
4	RNCS Relative negative charged SA (SAMNEG * RNCG) [Zefirov's PC]	Electrostatic descriptors
5	Max net atomic charge	Quantum descriptors

3.3 Model structure

The CAPSO BP ANN model was established with the molecular descriptors selected by CAPSO. The CAPSO BP ANN model adopted the three-layer structure composed of the input layer, the hidden layer, and the output layer. The input layer includes five input parameters representing the selected five molecular descriptors. The input parameters are: relative number of N atoms, Randic index (order 3), RNCG relative negative charged (QMNEG/QTMINUS) [Quantum-Chemical PC], RNCS relative negative charged SA (SAMNEG * RNCG) [Zefirov's PC] and Max net atomic charge. The output layer has one output parameter representing corresponding pKa value.

In this paper, the number of hidden layers is estimated with the formula: (2*sqrt(m*n)+1, where *m* and *n* are the number of the nodes of the input and output layers) and then the number of optimal hidden layer nodes is determined by the heuristic method. The model in this paper contains five input nodes and one output node, so the number of hidden layer nodes is estimated to be 5. Then, we assumed that the node of hidden layer is from 3 to 15, respectively. Fig.1 shows the comparison diagram of predicted error and the number of hidden layer nodes.

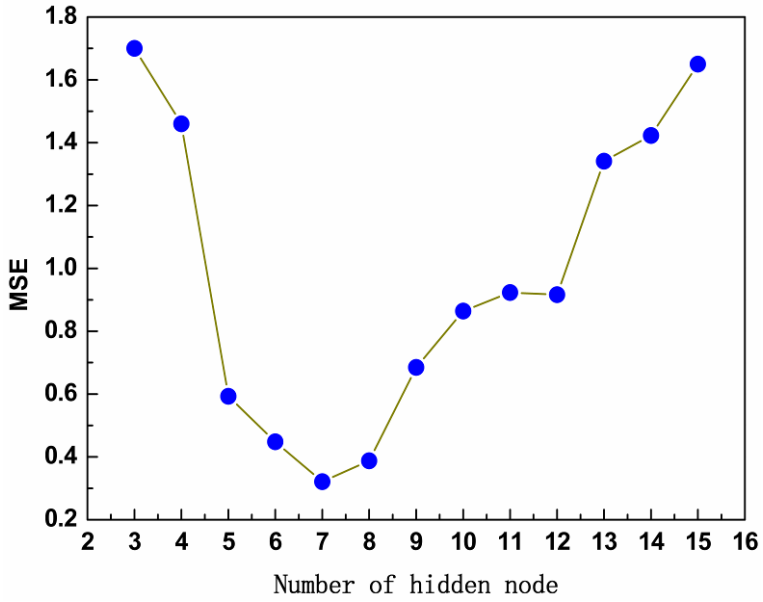

Fig.1 Optimization comparison diagram of the number of hidden layer nodes

As shown in Fig. 1, with the nodes number of hidden layer increasing, the trend of MSE decreasing first and then increasing. When the number is 7, the training MSE is the lowest and the structure of the prediction model is optimal. The model structure is 5-7-1.

4 Results and discussion

A three-layer (5-7-1) CAPSO BP ANN prediction model was established to predict the pKa value of the compound. First, the 188 and 40 sets of data from the training set and validation set were respectively used for model training and validation. Fig. 2 and Fig. 3 show comparison between the experimental value and the predicted value in the training set and validation set respectively. The circle and square respectively represent the predicted values of the model in the training set and the validation set, the vertical distances between the predicted data points and lines represent the absolute error of predicted values and experimental values.

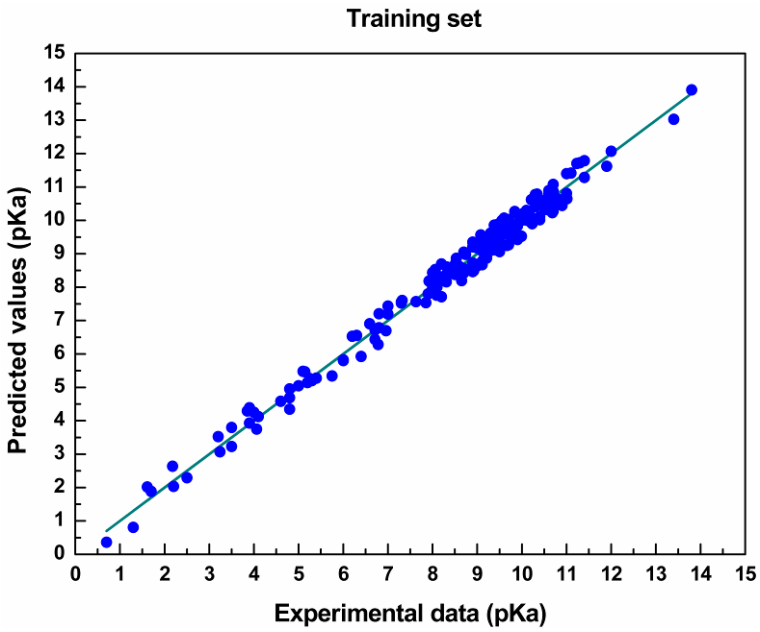

Fig.2 Comparison between the predicted and the experimental value in training set

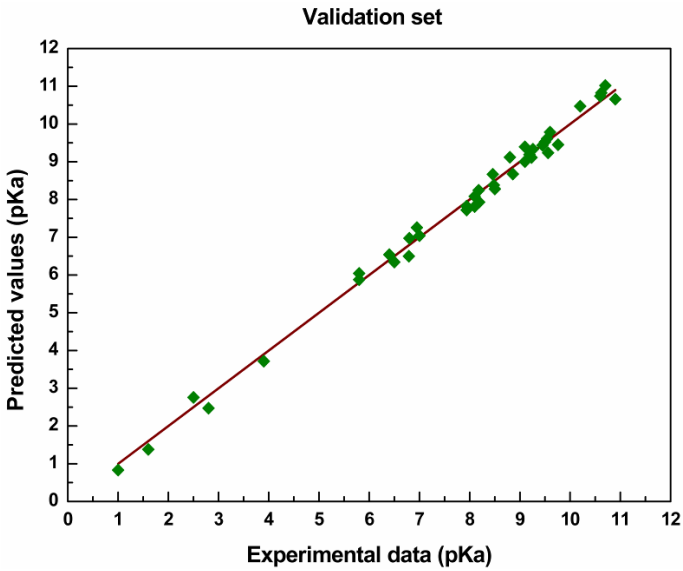

Fig.3 Comparison between the predicted and the experimental value in validation set

In the training set, the predicted value of model training is distributed around the actual value, indicating the high coincidence degree. From the vertical distance between the prediction data points and the line, we can see that the prediction error of the model is small and the prediction accuracy is high. In the validation set, the prediction results are significantly better than those in the training set, indicating that the training effect of the model is good.

Preprints (www.preprints.org) | NOT PEER-REVIEWED | Posted: 31 May 2018 doi:10.20944/preprints201805.0475.v1

Peer-reviewed version available at Appl. Sci. 2018, 8, 1121; doi:10.3390/app8071121

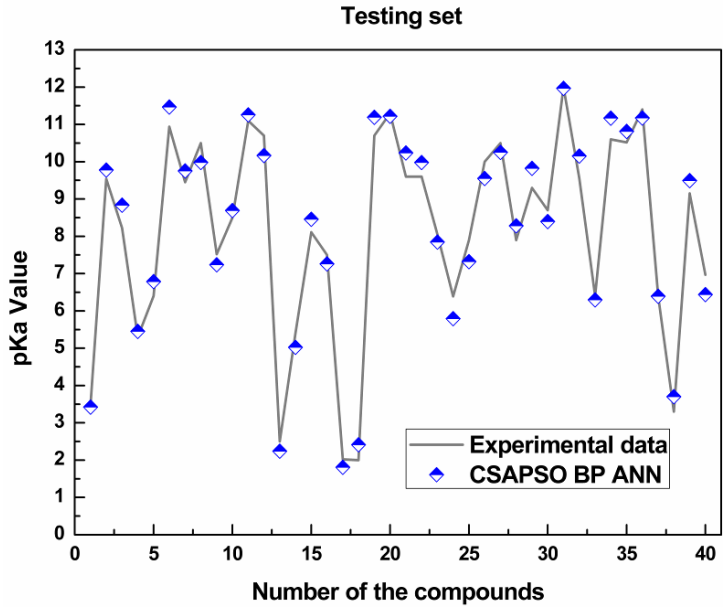

Fig. 4 Comparison between the predicted and the experimental value in testing set

Fig. 4 shows the correlation between the actual value and the predicted value of the model in testing set. In the testing set, the predicted value of the model is also in good agreement with the actual value. Table 3 shows the results of the model in the training set, validation set, and testing set.

Table 3 Statistics of model prediction performance

Set	*AARD*	*RMSEP*	R^2
Training	0.3436	0.0335	0.9771
Validation	0.3101	0.0211	0.9886
Testing	0.5364	0.0632	0.9438
Average	0.3967	0.0393	0.9698

The prediction results of the model in each subset are good and the prediction error is small, indicating the better comprehensive performance. The prediction performance of the model is better in terms of prediction accuracy and correlation. The above results prove that the prediction performance of the model is excellent.

In this study, three artificial intelligence models, BP ANN, SVM and PSO BP ANN, are selected as the comparison models. The prediction performance of the comparison model were compared with the PM3/COSMO method[34] . Figure 5 shows the prediction results of each model in testing set.

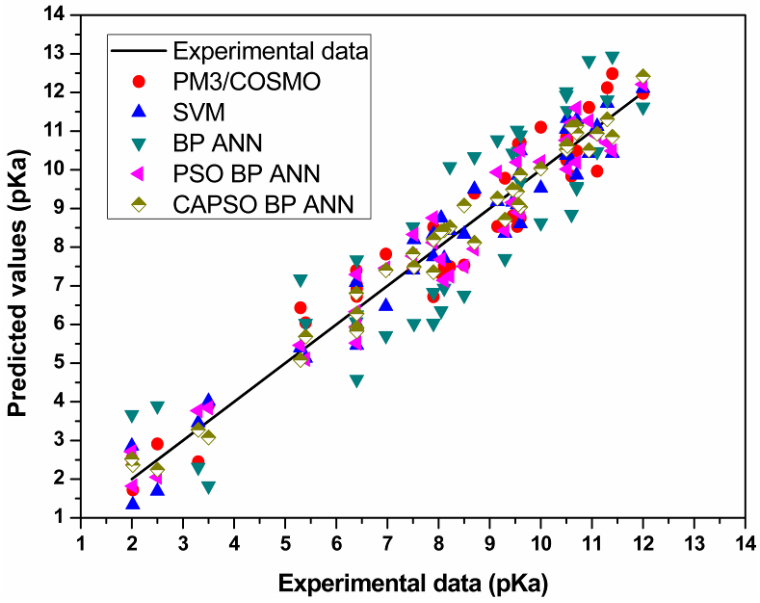

Fig. 5 Comparison of testing results of each model

As shown in Fig. 5, the vertical distance between the prediction data points and the experimental data show that the prediction data of CAPSO BP ANN model is near the experimental value, and the prediction performance proposed in this paper is obviously better than other methods. Fig. 6 is the residual curve between the experimental values and the predicted values of each model in testing set. Table 4 shows the evaluation results of each model.

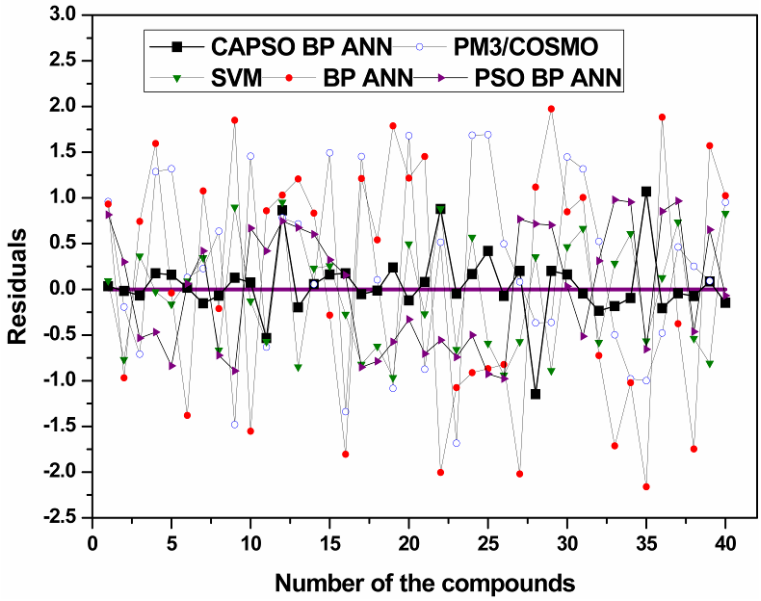

Fig. 6 Comparison of residual curves of testing results of each model

Table 4 Statistical results of each model

Model	*AARD*	*RMSEP*	R^2
PM3/COSMO	0.8724	0.1439	0.8346
SVM	0.7333	0.1038	0.8863
BP ANN	1.2134	0.5354	0.6958
PSO BP ANN	0.7229	0.1029	0.8872
CAPSO BP ANN	0.5364	0.0632	0.9438

It can be seen from the residual curve that the error of the model proposed in this paper is distributed near 0. Except some of the prediction points have large errors, the prediction error is better than other comparison models. the table shows that the accuracy and relevance of the CAPSO BP ANN model have obvious advantages. The performance of PM3/COSMO and SVM are equivalent to the PSO BP ANN model.

5. Conclusions

In this study, in order to solve the problem of molecular descriptor selection and model establishment in QSAR research, a novel chaos-enhanced accelerated particle swarm optimization algorithm (CAPSO) is proposed. The algorithm is applied in the selection of molecular descriptors and QSAR modeling and a prediction model called CAPSO BP ANN is obtained. Through the prediction experiment of the pKa values of compounds, the conclusions were drawn as follows:

The CAPSO algorithm could be applied in the selection of molecular descriptors. Prediction experiments showed that the five molecular descriptors selected by CAPSO algorithm could well represent the molecular structures of various compounds in the prediction of pKa value and provide the basis for the selection of molecular descriptors.

The CAPSO BP ANN model based on PSO algorithm and BP ANN had the good performance in the prediction experiment of the pKa values of various compounds and achieved the higher prediction accuracy and correlation. The experimental results showed that CAPSO BP ANN model could provide the basis for QSAR modeling.

Author Contributions: Mengshan Li conceived and designed the experiments. Mengshan Li, Bingsheng Chen and Huaijing Zhang wrote the main manuscript text. Yan Wu, Liang Liu and Lixin Guan analysed the data. All authors read and approved the final manuscript.

Funding: This research received no external funding.

Acknowledgments: The authors gratefully acknowledge the support from the National Natural Science Foundation of China (Grant Numbers: 51663001, 51463015, 61741103).

Conflicts of Interest: The authors declare no conflict of interest.

References

1. Cumming, J.G.; Davis, A.M.; Muresan, S.; Haeberlein, M.; Chen, H.M., Chemical predictive modelling to improve compound quality. *Nat. Rev. Drug Discovery* **2013**, *12*, 948-962, (10.1038/nrd4128).
2. Rojas, C.; Ballabio, D.; Consonni, V.; Tripaldi, P.; Mauri, A.; Todeschini, R., Quantitative structure-activity relationships to predict sweet and non-sweet tastes. *Theor Chem Acc* **2016**, *135*, 1-13, (10.1007/s00214-016-1812-1).
3. Patel, M.; Chilton, M.L.; Sartini, A.; Gibson, L.; Barber, C.; Covey-Crump, L.; Przybylak, K.R.; Cronin, M.T.D.; Madden, J.C., Assessment and reproducibility of quantitative structure-activity relationship models by the nonexpert. *J. Chem. Inf. Model.* **2018**, *58*, 673-682, (10.1021/acs.jcim.7b00523).
4. Liu, C.M.; Dou, X.W.; Zhang, L.; Kong, W.J.; Wu, L.; Duan, Y.P.; Yang, M.H., Development of a broad-specificity antibody-based immunoassay for triazines in ginger and the quantitative structure-activity relationship study of cross-reactive molecules by molecular modeling. *Anal Chim Acta* **2018**, *1012*, 90-99, (10.1016/j.aca.2018.01.042).
5. Gebreyohannes, S.; Dadmohammadi, Y.; Neely, B.J.; Gasem, K.A.M., A comparative study of qspr generalized activity coefficient model parameters for vapor-liquid equilibrium mixtures. *Ind Eng Chem Res* **2016**, *55*, 1102-1116, (10.1021/acs.iecr.5b03858).
6. Dardonville, C.; Caine, B.A.; Navarro de la Fuente, M.; Martin Herranz, G.; Corrales Mariblanca, B.; Popelier, P.L.A., Substituent effects on the basicity (pk(a)) of aryl guanidines and 2-(arylimino) imidazolidines: Correlations of ph-metric and uv-metric values with predictions from gas-phase ab initio bond lengths. *New J Chem* **2017**, *41*, 11016-11028, (10.1039/c7nj02497e).
7. Pandit, A.; Sengupta, S.; Krishnan, M.A.; Reddy, R.B.; Sharma, R.; Venkatesh, C., First report on 3d-qsar and molecular dynamics based docking studies of gcpii inhibitors for targeted drug delivery applications. *J Mol Struct* **2018**, *1159*, 179-192, (10.1016/j.molstruc.2018.01.059).
8. Shahlaei, M., Descriptor selection methods in quantitative structure-activity relationship studies: A review study. *Chem Rev* **2013**, *113*, 8093-8103, (10.1021/cr3004339).
9. Barley, M.H.; Turner, N.J.; Goodacre, R., Improved descriptors for the quantitative structure-activity relationship modeling of peptides and proteins. *J. Chem. Inf. Model.* **2018**, *58*, 234-243, (10.1021/acs.jcim.7b00488).
10. Soper-Hopper, M.T.; Petrov, A.S.; Howard, J.N.; Yu, S.S.; Forsythe, J.G.; Grover, M.A.; Fernandez, F.M., Collision cross section predictions using 2-dimensional molecular descriptors. *Chem Commun* **2017**, *53*, 7624-7627, (10.1039/c7cc04257d).
11. Khajeh, A.; Modarress, H.; Zeinoddini-Meymand, H., Application of modified particle swarm optimization as an efficient variable selection strategy in qsar/qspr studies. *J Chemometr* **2012**, *26*, 598-603, (10.1002/cem.2482).
12. Li, M.S.; Liu, L.; Huang, X.Y.; Liu, H.S.; Chen, B.S.; Guan, L.X.; Wu, Y., Prediction of supercritical carbon dioxide solubility in polymers based on hybrid artificial intelligence method integrated with the diffusion theory. *RSC Adv.* **2017**, *7*, 49817-49827, (10.1039/c7ra09531g).
13. Liu, Q.Z.; Wang, S.S.; Li, X.; Zhao, X.Y.; Li, K.; Lv, G.C.; Qiu, L.; Lin, J.G., 3d-qsar, molecular docking, and oniom studies on the structure-activity relationships and action mechanism of nitrogen-containing bisphosphonates. *Chem Biol Drug Des* **2018**, *91*, 735-746, (10.1111/cbdd.13134).
14. Wang, N.N.; Dong, J.; Deng, Y.H.; Zhu, M.F.; Wen, M.; Yao, Z.J.; Lu, A.P.; Wang, J.B.; Cao, D.S., Adme properties evaluation in drug discovery: Prediction of caco-2 cell permeability using a combination of nsga-ii and boosting. *J. Chem. Inf. Model.* **2016**, *56*, 763-773, (10.1021/acs.jcim.5b00642).
15. Fujita, T.; Winkler, D.A., Understanding the roles of the "two qsars". *J. Chem. Inf. Model.* **2016**, *56*, 269-274, (10.1021/acs.jcim.5b00229).

16. Borisek, J.; Drgan, V.; Minovski, N.; Novic, M., Mechanistic interpretation of artificial neural network-based qsar model for prediction of cathepsin k inhibition potency. *J Chemometr* **2014**, *28*, 272-281, (10.1002/cem.2617).
17. Du, X.J.; Wang, J.L.; Jegatheesan, V.; Shi, G.H., Dissolved oxygen control in activated sludge process using a neural network-based adaptive pid algorithm. *Appl Sci-Basel* **2018**, *8*, (10.3390/app8020261).
18. Verma, R.P.; Matthews, E.J., Estimation of the chemical-induced eye injury using a weight-of-evidence (woe) battery of 21 artificial neural network (ann) c-qsar models (qsar-21): Part i: Irritation potential. *Regul Toxicol Pharm* **2015**, *71*, 318-330, (10.1016/j.yrtph.2014.11.011).
19. Yasrab, R.; Gu, N.J.; Zhang, X.C., An encoder-decoder based convolution neural network (cnn) for future advanced driver assistance system (adas). *Appl Sci-Basel* **2017**, *7*, (10.3390/app7040312).
20. Selzer, D.; Neumann, D.; Schaefer, U.F., Mathematical models for dermal drug absorption. *Expert Opin. Drug Metab. Toxicol.* **2015**, *11*, 1567-1583, (10.1517/17425255.2015.1063615).
21. Hassanzadeh, Z.; Kompany-Zareh, M.; Ghavami, R.; Gholami, S.; Malek-Khatabi, A., Combining radial basis function neural network with genetic algorithm to qspr modeling of adsorption on multi-walled carbon nanotubes surface. *J Mol Struct* **2015**, *1098*, 191-198, (10.1016/j.molstruc.2015.05.039).
22. Dolara, A.; Grimaccia, F.; Leva, S.; Mussetta, M.; Ogliari, E., Comparison of training approaches for photovoltaic forecasts by means of machine learning. *Appl Sci-Basel* **2018**, *8*, (10.3390/app8020228).
23. Kennedy, J.; Eberhart, R., Particle swarm optimization. In *1995 IEEE International Conference on Neural Networks Proceedings, Proceedings of ICNN'95 - International Conference on Neural Networks*, IEEE Australia Council: Perth, 1995; Vol. 4, pp 1942-1948.
24. Wang, F.; Zhou, L.D.; Wang, B.; Wang, Z.; Shafie-Khah, M.; Catalao, J.P.S., Modified chaos particle swarm optimization-based optimized operation model for stand-alone cchp microgrid. *Appl Sci-Basel* **2017**, *7*, (10.3390/app7080754).
25. Liang, C.H.; Tong, X.M.; Lei, T.Y.; Li, Z.X.; Wu, G.S., Optimal design of an air-to-air heat exchanger with cross-corrugated triangular ducts by using a particle swarm optimization algorithm. *Appl Sci-Basel* **2017**, *7*, (10.3390/app7060554).
26. Gandomi, A.H.; Yun, G.J.; Yang, X.S.; Talatahari, S., Chaos-enhanced accelerated particle swarm optimization. *Commun Nonlinear Sci* **2013**, *18*, 327-340, (10.1016/j.cnsns.2012.07.017).
27. Jiang, G.W.; Luo, M.Z.; Bai, K.Q.; Chen, S.X., A precise positioning method for a puncture robot based on a pso-optimized bp neural network algorithm. *Appl Sci-Basel* **2017**, *7*, (10.3390/app7100969).
28. Yang, X.S.; Deb, S.; Fong, S., Accelerated particle swarm optimization and support vector machine for business optimization and applications. In *Networked digital technologies*, Fong, S., Ed. Springer-Verlag Berlin: Berlin, 2011; Vol. 136, pp 53-66.
29. Han, F.; Zhu, J.S., Improved particle swarm optimization combined with backpropagation for feedforward neural networks. *Int J Intell Syst* **2013**, *28*, 271-288, (10.1002/int.21569).
30. Li, M.S.; Zhang, H.J.; Chen, B.S.; Wu, Y.; Guan, L.X., Prediction of pka values for neutral and basic drugs based on hybrid artificial intelligence methods. *Sci Rep* **2018**, *8*, (10.1038/s41598-018-22332-7).
31. Zolfaghari, S.; Noor, S.B.M.; Mehrjou, M.R.; Marhaban, M.H.; Mariun, N., Broken rotor bar fault detection and classification using wavelet packet signature analysis based on fourier transform and multi-layer perceptron neural network. *Appl Sci-Basel* **2018**, *8*, (10.3390/app8010025).
32. Valdez, F.; Melin, P.; Castillo, O., Modular neural networks architecture optimization with a new nature inspired method using a fuzzy combination of particle swarm optimization and genetic algorithms. *Inform Sciences* **2014**, *270*, 143-153, (10.1016/j.ins.2014.02.091).
33. Li, N.J.; Wang, W.J.; Hsu, C.C.J.; Chang, W.; Chou, H.G.; Chang, J.W., Enhanced particle swarm optimizer incorporating a weighted particle. *Neurocomputing* **2014**, *124*, 218-227, (10.1016/j.neucom.2013.07.005).
34. Jensen, J.H.; Swain, C.J.; Olsen, L., Prediction of pk(a) values for druglike molecules using semiempirical quantum chemical methods. *J Phys Chem A* **2017**, *121*, 699-707, (10.1021/acs.jpca.6b10990).
35. Eckert, F.; Klamt, A., Accurate prediction of basicity in aqueous solution with cosmo-rs. *J Comput Chem* **2006**, *27*, 11-19, (10.1002/jcc.20309).
36. Luan, F.; Ma, W.P.; Zhang, H.X.; Zhang, X.Y.; Liu, M.C.; Hu, Z.D.; Fan, B.T., Prediction of pk(a) for neutral and basic drugs based on radial basis function neural networks and the heuristic method. *Pharmaceut Res* **2005**, *22*, 1454-1460, (10.1007/s11095-005-6246-8).